

HIGH PERFORMANCE SASE FEL ACHIEVED BY STABILITY-ORIENTED ACCELERATOR SYSTEM

H. Tanaka[#], T. Fukui, T. Hara, N. Hosoda, T. Inagaki, S. Inoue, T. Ishikawa, H. Kitamura, N. Kumagai, C. Kondo, H. Maesaka, M. Nagasono, T. Ohshima, Y. Otake, T. Sakurai, T. Shintake, T. Tanaka, K. Togawa, K. Tono, M. Yabashi, RIKEN/SPring-8, Hyogo, Japan
 T. Hasegawa, Y. Kano, T. Morinaga, H. Ohashi, Y. Tajiri, K. Shirasawa, S. Takahashi, S. Tanaka, T. Togashi, M. Yamaga, R. Yamamoto, JASRI/SPring-8, Hyogo, Japan

Abstract

A stable Self-Amplified Spontaneous Emission (SASE) Free-Electron Laser (FEL) has been routinely used for user experiments since May 2008 at the SPring-8 Compact SASE Source (SCSS) test accelerator. In FY2008, a beam time of 840 hr (95 days) was provided to 11 research groups with a small downtime rate of ~4%. In spite of day-by-day operation, FEL radiation properties, which include a pulse energy of ~30 μ J with an intensity fluctuation of 10~15% in STD at wavelengths from 50 to 60 nm, have been readily reproducible without a complicated beam feedback control. These stability and reproducibility, which were originally targeted in the system design, have been highly improved by continuous R&D activities of the system components and operational efforts that eliminate error sources causing FEL instability.

INTRODUCTION

An FEL emits spatially and temporally coherent radiation by wiggling a brilliant (low-emittance and high peak-current) electron beam in an alternate magnetic field with a large number of periods. Since FEL performance strongly depends on a density distribution of the electron beam in the six-dimensional phase space, stability of this density distribution is critically important for stable FEL operation. It is, however, difficult to stabilize the shot-by-shot beam density distribution in a linac-based FEL which is an open-loop system without an autonomous stabilization mechanism [1]. Phase and amplitude variations of each rf acceleration structure in a bunch compression system directly change the beam density distribution. This situation is completely different from that of a ring-based synchrotron radiation (SR) source where a Gaussian-like beam density distribution is formed through the dynamical equilibrium between the radiation excitation (noise) and the radiation damping. How to achieve stable FEL operation with the linac-based machine is one of the biggest issues towards the practical use of SASE FELs.

Aiming at achieving a stable and high performance SASE FEL, a unique X-ray FEL (XFEL) facility [2,3] based on a SCSS concept [4,5] is under construction at SPring-8, Japan. Prior to the XFEL construction, the SCSS test accelerator was built to demonstrate high performance of the FEL system based on the SCSS

concept [6,7]. A schematic drawing of the test accelerator is shown in Fig. 1.

At the beginning, the SASE lasing was not so stable to integrate multiple steps required for precise beam tuning. The causes of the instability had been experimentally investigated and eliminated one-by-one since autumn 2006. The precise tuning became feasible after stabilizing the electron gun and rf system in the injector, making the SASE lasing reproducible in summer 2007. The replacement of the 2nd undulator enabled us to observe the first evidence for power saturation of a SASE FEL in the Extremely Ultra-Violet (EUV) region in autumn 2007 [8-10], which had proved the validity of the system. Further efforts to suppress a drift of the SASE FEL power in 2008 [11] brought the continuous power saturation of a SASE FEL was obtained with good reproducibility. The resultant stable SASE-FEL has been offered to user experiments since May 2008.

In this paper are described the keys for a stable FEL system at the beginning, followed by the review of main R&D activities and operational efforts to achieve the stabilization realizing the continuous power saturation. Finally, the currently achieved laser performance and operationability are summarized.

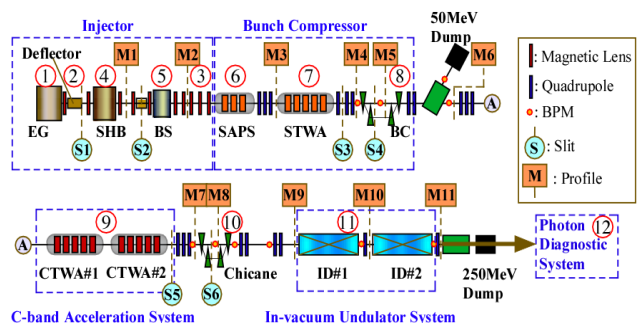


Figure 1: Schematic drawing of the SCSS test accelerator. 1, 500-kV pulsed electron gun (EG); 2, deflector; 3, magnetic lenses; 4, 238-MHz sub-harmonic buncher (SHB); 5, 476-MHz booster cavity (BS); 6, S-band APS cavity (SAPS); 7, S-band travelling-wave acceleration structure (STWA); 8, bunch compressor (BC); 9, C-band acceleration system (CTWA#1&CTWA#2); 10, chicane; 11, in-vacuum undulator system (ID#1 & ID#2); and 12, photon diagnostic system.

[#]tanaka@spring8.or.jp

KEY POINTS FOR STABLE FEL SYSTEM

Below we list essential issues for achieving a stable FEL system:

- Reproducibility.
- Simplicity.
- Low perturbation-noise.
- Reliability.
- Maintainability.

Key points for approaching these targets are (a) high stability of the electron source and (b) thorough suppression of high frequency noise (perturbation). For the former, the initial condition of the electron beam, which never smears out through the beam acceleration, determines the final beam quality. Development of a reliable electron gun reproducing the stable electron beam is necessary for stable FEL operation. For the latter, high frequency noise up to a few tens MHz, which is introduced by a linac rf system and cannot be corrected by a beam feedback, seriously modulates the beam current distribution. Suppression of the high frequency noise is thus crucial for the stable operation.

R&D FOR STABLE ELECTRON SOURCE

Presently two types of electron guns are available for SASE-FEL application; photo-cathode rf and pulsed-thermionic guns. Although both could provide a high-quality electron beam, a thermionic gun was adopted for the XFEL at SPring-8 on the basis of the following stability-related reasons.

Simplicity and Tunability

The laser-driven photo-cathode rf gun can efficiently generate an intense short-pulsed electron beam. However, dynamics of the electron beam in the gun is quite complicated, i.e., governed by a three-dimensional (3-D) space charge effect, acceleration, bunching and transversal focusing effects due to a 3-D rf electromagnetic field. The photo-cathode rf gun is required to control these multiple parameters for handling the electron beam. On the other hand, the functions are separately allocated for each component in the system based on the pulsed-thermionic gun. Here, the gun only generates a mono-energetic uniform beam and the following deflector only slices out a short-pulsed beam from the long pulse. Then, sub-harmonic buncher generates an energy chirp over the bunch for bunch compression and so forth. This design enables one to facilitate the beam tuning and to improve the tuning reproducibility with an operation flexibility.

Electron Beam Homogeneity

A laser-induced photoemission process used in the photo-cathode rf gun has a fast time-response as to generate an intense and short-pulsed electron beam. The beam distribution thus naturally reflects on the drive-laser intensity fluctuation in time and in space. When the electron beam has once a spiky intensity modulation, this modulation grows up passing through the accelerator,

especially in bunch compressors. Therefore, the stable FEL operation requires the stable drive-laser without high frequency fluctuations. On the other hand, in the case of a thermionic gun, spatial and temporal homogeneity of the electron beam is determined by the cathode surface-flatness and temperature distribution over the cathode. Since thermal-conductive properties smear out high frequency temperature variations, the spiky density modulation can be eliminated by selecting an adequate single crystal as the cathode material.

500-kV Pulsed Thermionic Electron Gun with a CeB₆ single Crystal Cathode

A pulsed thermionic gun with a CeB₆ single crystal cathode was developed to generate a homogeneous, clean and low-emittance electron beam [5,12].

The cathode of which the diameter is 3 mm is buried in a graphite sleeve to reduce beam halo. It is heated up to ~1800 K by a graphite heater surrounding the sleeve. Flat electrodes were adopted to reduce emittance growth and to enlarge a dynamic range of the extraction current. A gap distance of 50 mm between the cathode and the anode was determined to operate the gun in the temperature-limited region. A control grid was also removed from the cathode to maintain the beam homogeneity and low-emittance. To reduce the space charge effect a high voltage of 500 kV was selected. This high beam energy allows us to simplify the beam motion by removing a conventional solenoid coil covering a buncher section. Normalized emittance of 0.6π mm mrad was experimentally obtained as a 90% core part in the performance test [12].

The developed gun system had been successfully operated in the SCSS test accelerator with cathode heating time of about 20,000 hours with nearly maintenance-free condition. Since the target value of the gun peak current, 1 A, became unattainable in January 2008, the cathode assembly was replaced by new one. After the replacement, the stable power saturation of a SASE FEL was successfully reproduced. The replacement of the cathode assembly took one week with raising the cathode temperature and extraction voltage up to the nominal operation values. Since the cathode assembly replacement, the electron gun has been operated for about one and half year without any maintenance. Figure 2 and



Figure 2: Scene in the replacement of the gun cathode.

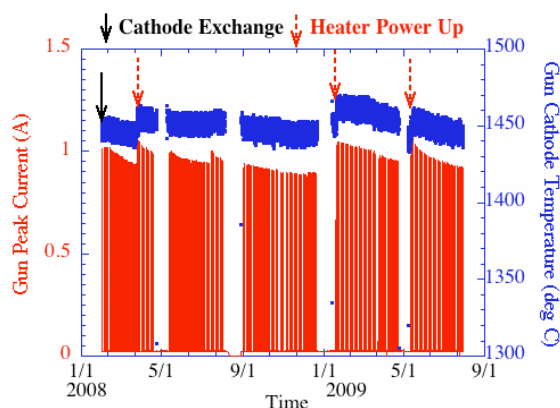


Figure 3: Peak current variation of the new cathode over recent one and half year.

3 show the one scene in the cathode assembly replacement and the gun peak current variation after the replacement, respectively.

R&D FOR HIGH FREQUENCY NOISE SUPPRESSION

The R&D activities are summarized below, which mainly contributed to realization of the stable FEL operation. More detailed information can be found in Ref. 3 and 15.

Klystron Modulator Power Supply with High Precision

Sensitivity analysis of the peak current on the RF amplitude and phase variations [13,14] showed that required voltage stability of the pulse forming network (PFN) in the modulator is 100 ppm in peak-to-peak value for the XFEL. However, achievable stability with the existing technologies was about 0.1%, by one-order higher than the requirement.

A klystron modulator power supply having stability better than 100 ppm has been therefore developed on the basis of a feedback control [15]. The power supply has a feedback loop where a control target is a PFN voltage and a control valuable is a charging current on the target. Key points in the development are the following two:

- A high-voltage probe with sufficiently fast time response and high accuracy.
- High resolution of the charging voltage

A new 50-kV high-voltage probe with a fast time response and a low thermal drift was developed by JAPAN FINECHEM COMPANY, Inc. [16]. The fast time response was obtained by reducing resistance of the probe. The resultant larger heat dissipation was solved by adopting (a) a resistor with a low thermal coefficient and (b) a fluorinert-filled casing with a cooling water pipe. For the high resolution of the charging voltage, a special design was introduced to satisfy both a wide dynamic range and high resolution using two units with different

charging speeds and capacities. The power supply has two inverter units in parallel. One is a high capacity inverter called “main charger” with 2 A output for high speed charging, and the other is a low capacity inverter called “sub charger” with a two-order smaller output for high-precision charging. After the main charger charges up to about 99.7% of the target voltage, the sub charger then precisely charges the remaining voltage. In 2008 NICHICON CORPORATION manufactured a klystron modulator power supply with high precision [17] based on the above concept. Figure 4 shows a typical waveform of the charging cycle. The voltage jitter found to be 60 ppm in peak-to-peak (10 ppm in STD), which satisfies the requirement for the XFEL. The previous versions with a voltage jitter of 30 ppm in STD are now used in the SCSS test accelerator, which will be replaced by the final ones in the near future.

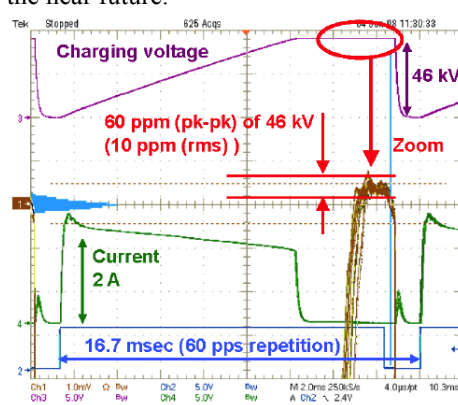


Figure 4: Typical waveform of the charging cycle and the charging voltage stability.

Compact Oil-Filled Modulator

A compact and high performance modulator was developed as a common pulsed power source to drive the C-band klystron, the S-band Klystron and the 500-kV pulsed electron gun [5,18]. This modulator can supply a peak power of 114 MW at a maximum repetition rate of 60 pps. All high-voltage (HV) components of the modulator including a PFN circuit, a thyatron tube and a reflected voltage clippers are contained in a steel tank filled with insulating oil. Four modulators of this type are operated in the SCSS test accelerator. The developed modulator used for the 2nd C-band acceleration unit is shown in Fig. 5. In a final design, two oil-filled tanks, one of which is for the modulator and the other is for the pulse transformer, were unified into the single tank. From the viewpoint of stable FEL operation, the developed modulator has the following advantages: (a) Since the stainless steel tank contains all electro-magnetic (EM) noise sources, most of EM noise from the modulator is efficiently shielded. (b) HV circuits are perfectly free from the humidity and dust, which often cause the leakage current and discharge. (c) The unified single tank reduces HV cables and connectors, which often cause HV breakdown.

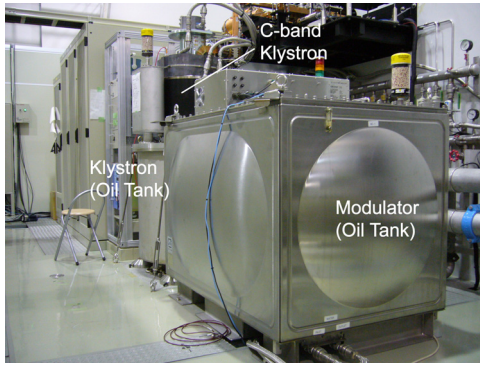


Figure 5: Compact oil-filled modulator.

Stable and Low Noise Master Oscillator

A stable and low noise master oscillator (MO) is an essential sub-system for a precise timing system with a precision of a few tens femto-second, and also contributes to suppression of the high frequency rf perturbations. A MO was developed on the basis of sequential down-conversion of reference signal frequencies by frequency dividers [19]. A feature of the developed MO is low single sideband (SSB) noise over a whole frequency range.

Figure 6 shows a circuit diagram of the developed MO. All sinusoidal reference signals are made of the 2856 MHz signal source (SS) by using a frequency doubler and frequency dividers. On the other hand, a conventional scheme generates all necessary frequencies from a single sub harmonic using frequency multipliers. In every multiplication step, the integrated noise power increases according to the multiplication rate. It is therefore difficult to achieve a low SSB noise level for higher reference frequencies.

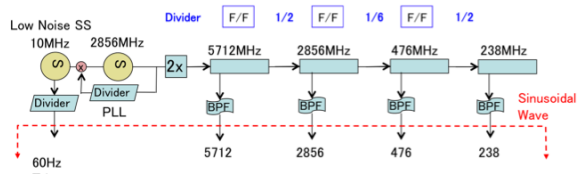


Figure 6: Circuit diagram of the developed MO.

The key point is to develop a sufficiently low noise SS at a rather high frequency of 2856 MHz. To solve this problem, the 2856-MHz SS is connected to the 10-MHz SS with a phase locked loop (PLL) as shown in Fig. 6. The 2856 MHz SS has a low-noise characteristic in a frequency range above ~1 kHz, while the 10 MHz SS has a low-noise characteristics in the range below ~1 kHz. By connecting the two sources with a PLL, the low-noise frequency range can be effectively expanded.

Consequently, the SSB noise is reduced over a full frequency range as shown in Fig. 7. We see in the figure that the achieved noise level is -140 dBc at 1 MHz. The timing control system for the SCSS test accelerator was constructed using the developed MO, a VME master

trigger module, a differential trigger pulse transmission system and other components [19]. To confirm stability of the timing control system, the bunch arrival time was measured shot-by-shot by using a cavity-type beam position monitor (BPM) installed downstream of the C-band acceleration system. The measured time jitter was 46 fs in STD showing the sufficient performance for the XFEL [20].

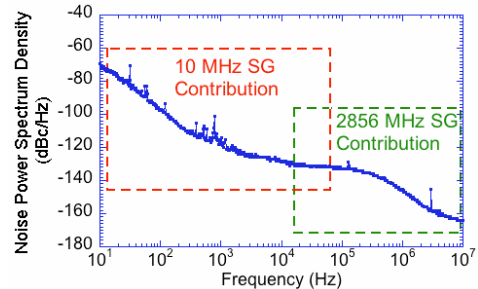


Figure 7: SSB noise power spectrum density of the MO.

Precise Control of RF Phase and Amplitude

Tolerances of an RF phase and amplitude for the XFEL are 100 femto seconds in time (~0.1 deg at a S-band frequency) and 0.01%, respectively. These are determined so as to achieve stable SASE saturation at the X-ray regime. In order to meet the requirements, the low-level rf (LLRF) system was developed and tested in the SCSS test accelerator [21,22]. The LLRF system consists of in-phase and quadrature-phase (IQ)-modulators/demodulators and VME waveform generator (A/Ds)/digitizers (D/As). Features of the developed system are:

- Fast time response.
- High setting and reading resolution.
- Programmable setting.

Pickup signal-based PLLs and auto level controls (ALCs) were built to suppress the rf phase and amplitude drifts by using the developed system and a PID control algorithm. After the following two improvements, we have achieved the stabilities as shown in Fig. 8, which show potentiality to satisfy the requirements for the XFEL by further improvements: (a) The temperature of the cavity bodies has been stabilized within 10 mK by improving the control of the cooling water system. (b) A

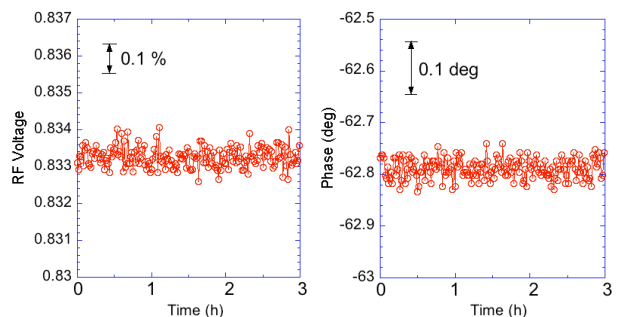


Figure 8: Achieved phase and amplitude stabilities of the 476-MHz booster cavity after improvements.

waveform dithering method was introduced, which varies a parameter value during the cavity filling time and effectively improves the resolutions of the integrated setting parameters [11,21,22]. The dithering method is at present unnecessary because the setting resolution was sufficiently raised by 14-bit D/As.

BEAM FEEDBACK TOWARDS STABLE FEL

Two beam feedback loops have been developed in the SCSS test accelerator aiming at realization of the stable XFEL. One is an orbit drift correction over an undulator section and the other is a correction of a beam current distribution.

Correction of Orbit Drift

The correction objects are presently restricted to the orbit displacements measured by BPMs in the undulator section. Since the beam operation is performed day-by-day, the operation period is short, basically only nine hours. It is therefore assumed that the orbit distortion over the undulator section for this short period is caused by the variation of some parameters of the upstream RF system, never by the position drifts of quadrupoles in the undulator section. This assumption simplifies the correction scheme into two stages. The horizontal and vertical positions are corrected first at the entrance of the undulator section by using the upstream single steering magnets. The angle errors are then corrected in both planes by the single steering magnets just downstream of the BPM used in the first stage to minimize the displacements over the undulator section. It is clear that the two corrections are decoupled by the adequate steering choice. The correction is currently performed with a cycle of 0.2 Hz by using the orbit estimated by averaging 45 shot-by-shot data [24]. By this correction, the horizontal and vertical orbit drifts have been reduced down to 6.4 and 2.3 μm , respectively. The rather large horizontal drift is due to the leakage of a horizontal dispersion from the upstream chicane, which will be corrected in the XFEL. Figure 9 shows the vertical orbit

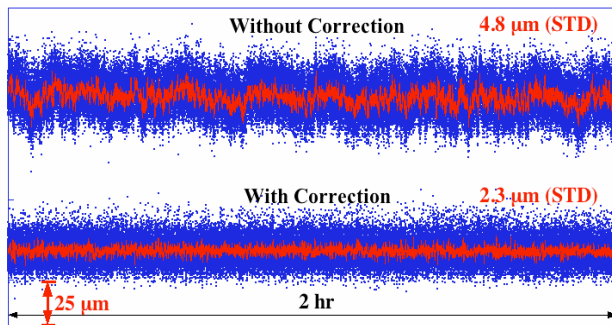


Figure 9: Vertical orbit drifts over 2 hours with and without the correction. The blue dots and the red lines represent the shot-by-shot data and moving-averaged orbit with the 45 data. The measurement position is the middle of the undulator section.

drifts between the two undulators over 2 hours with and without the correction. To apply this feedback correction to the XFEL we have been investigating acceleration of the correction cycle speed up to 1 Hz and an additive correction algorithm for the orbit distortion by the dipole errors located in the undulator section.

Correction of Beam Current Distribution

The XFEL at SPring-8 has a multiple-stage bunch compression system composed of a velocity bunching and following three magnetic-bunching processes. For achieving the stable SASE FEL, local beam feedback loops fixing the beam current distribution at the exit of each bunching process are crucial as demonstrated at LCLS [25]. Key points in the development are a feedback model for the velocity bunching and the separation between the velocity bunching and the first magnetic-bunching. In order to test the feedback model for the velocity bunching and stabilize SASE intensity further in the SCSS test accelerator, a simple feedback loop has been introduced, in which an energy variation of the magnetic-chicane is returned to a phase of the 238 MHz SHB [26]. Here, it is assumed that a voltage drift of the electron gun mainly causes the energy variation in such day-by-day operation. Figure 10 shows the SASE intensity and beam energy variations at the magnetic chicane with and without the correction. It is found that the energy-correlated SASE intensity variation is suppressed to some extent by the correction. In order to complete the two-stage feedback loops for stabilizing the beam current distribution, a beam arrival timing detection system will be installed in this summer. An intensity detection system of coherent THz SR will be also built from this autumn to monitor bunch length variation.

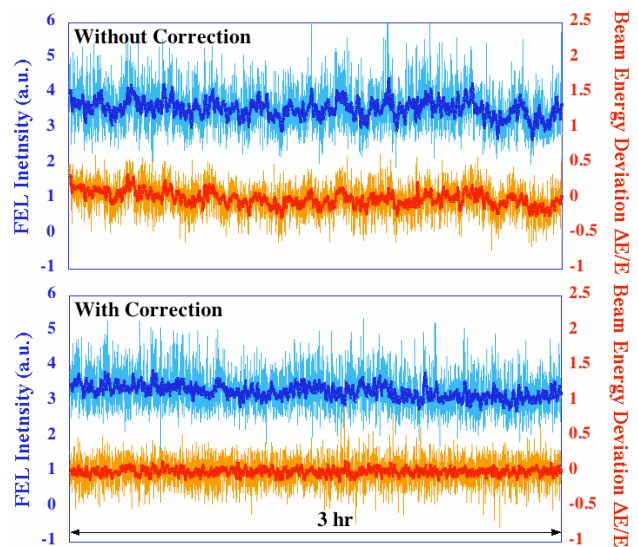


Figure 10: Shot-by-shot SASE intensity and beam energy variations at the magnetic chicane over 3 hours with and without the feedback correction. The blue and red bold lines represent the moving-averaged variables with 20 shot-by-shot data.

ACHIEVED LASER PERFORMANCE AND OPERATIONABILITY

The continuous power saturation of a SASE FEL has been routinely obtained due to the elaborate efforts on the accelerator stabilization. In FY2008, a total beam time is 1941 hr (200 days) and its 43%, 840 hr (95 days) was provided to 11 research groups covering research fields of atomic, molecular, and optical (AMO) science, coherent imaging, ultra-fast laser spectroscopy, plasma science, and material science. A downtime rate for the user beam time was ~4%. The regular beam time in a day is currently 9 hr from 10:00 AM to 7:00 PM.

Laser Performance at User Experiments

The achieved SASE FEL performance is listed in Table 1. Experimental users can freely select the using wavelength between 50 and 60 nm by changing the undulator gap. For utilizing longer wavelengths than 60 nm, some machine study period, 2~3 days, are required to prepare the machine parameter-set for lower energy operation. The resolution of the delivered laser wavelength is about 0.1 nm. The necessary time for changing a wavelength is about 20 minutes including the laser intensity and wavelength checks and the laser beamline setting procedures. The minor wavelength change of ~several tenth nm is possible without interrupting the experiment, which only takes a few minutes.

Table 1: Achieved SASE FEL performance.

Item	Achieved value
Wavelength	50~60 nm
Laser Pulse Energy	30~40μJ
Repetition Rate	20 Hz (60 Hz ^{*1})
Pulse Energy Fluctuation (STD)	~10%, 14~15% ^{*2}
Laser Profile Radius (FWHM) ^{*3}	3 mm
Pointing Stability ^{*3}	~5% of Laser Radius
Average Spectrum Width (FWHM)	0.6~1%

*1 60 Hz was tested only in the machine study.

*2 ~10% is for a short period and 14~15% is over the beam operation.

*3 16-m downstream of the source point.

All the laser pulses have high spatial coherence. In fact, we observe high-contrast fringes from the orifice edge (inner diameter = 10 mm), which is installed for differential pumping in the upstream laser beamline, for every single shot. Recently the diffraction imaging experiment verified the high spatial coherence of all the shots by the fact that all diffraction data measured have quality high enough for the analysis of phase retrieval.

Although we have presently no information on the laser pulse duration and its stability, variations of the electron beam temporal profiles were measured by the rf zero-

phasing method [27]. Figure 11 shows the ten temporal profiles measured with a sampling speed of 1 Hz. The peak current variation in two measurements is 2~5% in STD, which is consistent with a predicted value of 8% by Monte Carlo simulation using the measured rf phase and amplitude variations [10].

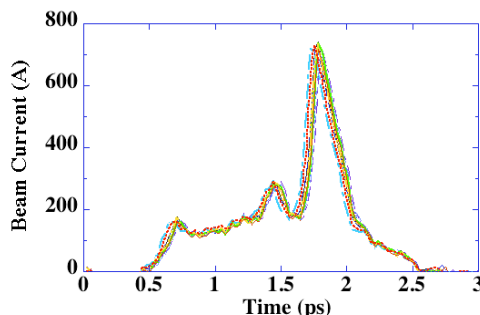


Figure 11: Temporal profile of electron beam.

By increasing the peak current from 300 A to ~700 A as shown in Fig. 11 the laser pulse energy has been increased especially in shorter wavelengths. A pulse energy of 30 μJ is available at any wavelength between 50 and 60 nm. The laser intensity is also adjustable depending on the user request. The accelerator side provides the stable laser with the small intensity fluctuation shown in Table 1. The gas attenuator [28] in the experimental hall attenuates the laser intensity to an arbitrary level. This high stability enables users to perform intensity-dependent measurement in real-time without any post-processing, e.g., data sorting. Currently, the laser pulse repetition rate is limited up to 20 Hz and 1, 5, 10 and 20 Hz are selectable as the repetition rate.

Figure 12 shows a transverse distribution of the laser in the experimental hall. The used Ce:YAG screen locates 16-meter downstream from the source point. The laser profile is symmetric, nearly bi-Gaussian with a diameter of ~6 mm in FWHM.

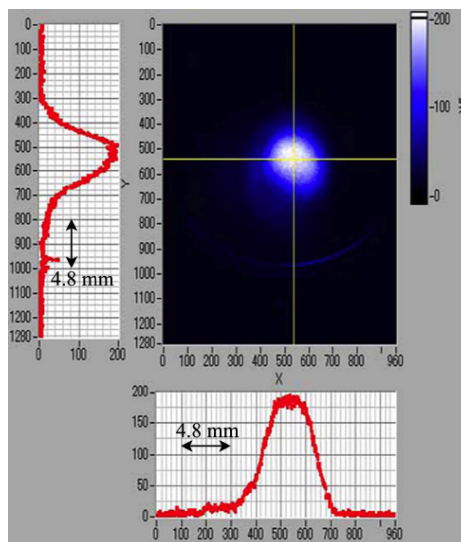


Figure 12: Laser transverse profile.

Machine Operationability

The beam operation is performed for 9 hr per day from 10:00 AM to 7 PM and for 5 days per week from Monday to Friday. The accelerator system is shut down over weekend except for a cathode heater of the thermionic gun. Every weekday morning, “low voltage” is turned on at 6:00 AM. In this procedure, the klystron cathode heaters and a cathode heater of the dummy tube are switched on in Monday or their power levels are raised up to the full in other weekday. The dummy tube is used for impedance matching between the gun cathode and the modulator instead of a real resistor. The various machine parameters drift over 3 hr. At 9:00 AM the drift is settled and then we start to patrol in the accelerator tunnel for closing the tunnel before operating the accelerator. Reloading the machine parameter usually reproduces the SASE FEL performance. The laser is typically delivered to the experimental hall at around 9:30 AM to adjust the laser positions, etc. Currently it takes one hour or less from starting the operation to deliver the laser to users. The regular beam operation for user experiments is fully automatic except when the machine fault is occurred. Frequency of the machine faults is about once a day in average. After the weekday operation, the accelerator system is kept in the “stand-by” condition where a heater power level of the cathode is reduced down to 25% at the operation.

Machine Troubles

We encountered three major troubles in 2006, at the beginning of the operation. One is a short circuit of the dummy tube cathode heater in the electron gun, which was a manufacturing defect. Initially there was little clearance between the uncoated heater power line and the metal reflector for thermal radiation. Next is a vacuum leakage of the S-band APS due to welding defects. These two troubles were resolved by the replacements. The last is an electric circuit damage of the klystron modulator power supply, which took a few months for repair. Since 2007, we have only experienced minor troubles such as short circuits of some power cables, failures of the solid-state amplifiers, failures of the thyratrons, etc. We exchanged thyratrons three times until now. Lifetimes of the exchanged thyratrons seem to be rather short. For this reason, we presently assume that the day-by-day operation gives larger thermal stress to the thyratrons compared with that by continuous 24-hr operation.

SUMMARY

After thorough suppression of the perturbation sources by improving the rf system stability and the beam operation a stable EUV SASE FEL keeping the power saturation over the operation period has been achieved in the SCSS test accelerator. This outstanding performance is reproducible even by day-by-day operation and maintained easily without serious troubles. Experience and results obtained by the user operation over more than one year reveals that the stability-oriented accelerator

system is effective for achieving the reliable and high performance SASE FEL.

REFERENCES

- [1] T. Shintake, in *Proceedings of FEL2004*, edited by R. Bakker, L. Giannessi, M. Maris, and R. Walker (Synchrotrone Trieste, Trieste, Italy, 2004), pp. 90–95.
- [2] SPring-8 Joint Project for XFEL, SPring-8 Research Frontiers 2007, edited by S. Kikuta (SPring-8 Document D2008-009, Japan Synchrotron Radiation Research Institute/SPring-8, Sayo, Japan, 2008), pp. 230–235.
- [3] Y. Otake, in *Proceedings of FEL2008*, Gyeongju, Korea, 2008 (Pohang Accelerator Laboratory, Pohang, Korea, 2009), pp. 222–226.
- [4] T. Shintake, H. Matsumoto, T. Ishikawa, and H. Kitamura, in *Proceedings of SPIE, Optics for Fourth-Generation X-Ray Sources*, edited by R. O. Tatchyn, A. K. Freund, and T. Matsushita (SPIE, Bellingham, WA, 2001), **Vol. 4500**, pp. 12–23.
- [5] SCSS X-FEL R&D Group, SCSS X-FEL Conceptual Design Report, edited by T. Shintake and T. Tanaka (RIKEN Harima Institute/SPring-8, Sayo, Japan, 2004).
- [6] T. Shintake and SCSS Group, in *Proceedings of the 10th European Particle Accelerator Conference*, edited by C. Biscari, H. Owen, Ch. Petit-Jean-Genaz, J. Poole, and J. Thomason (CCLRC Rutherford Appleton and Daresbury Laboratories, Edinburgh, Scotland, 2006), pp. 2741–2743.
- [7] H. Tanaka, K. Togawa, H. Baba, T. Hara, A. Higashiya, T. Inagaki, H. Maesaka, H. Matsumoto, K. Onoe, Y. Otake, K. Shirasawa, T. Tanaka, T. Tanikawa, M. Yabashi, and T. Shintake, in *Proceedings of FEL2006* (BESSY, Berlin, Germany, 2006), pp. 769–776.
- [8] T. Shintake et al., *Nature Photonics* 2, 555 (2008).
- [9] T. Tanaka et al., in *Proceedings of FEL2008*, Gyeongju, Korea, 2008 (Pohang Accelerator Laboratory, Pohang, Korea, 2009), pp. 537–542.
- [10] T. Shintake et al., *Physical Review ST-AB* 12, 070701 (2009).
- [11] H. Tanaka et al., in *Proceedings of the 11th European Particle Accelerator Conference*, edited by I. Andrian, O. Brüning, Ch. Petit-Jean-Genaz, and P. Pierini (INFN, ELETTRA, Sincrotrone Trieste, and CERN, Genoa, Italy, 2008), pp. 1944–1946.
- [12] K. Togawa, T. Shintake, T. Inagaki, K. Onoe, T. Tanaka, H. Baba, and H. Matsumoto, *Physical Review ST-AB* 10, 020703 (2007).
- [13] H. Tanaka, private communication, Internal report of XFEL/SPring-8.
- [14] J. S. Oh, T. Inagaki, K. Shirasawa, T. Hara, and T. Shintake, in *Proceedings of FEL2006* (BESSY, Berlin, Germany, 2006), pp. 684–687.
- [15] T. Inagaki et al., “8-GeV C-band Accelerator Construction for XFEL/SPring-8”, the 24th Linear

- Accelerator Conference (LINAC08), Victoria, British Columbia, Canada, 2008.
- [16] K. Okada, T. Ogawa, C. Kondo, T. Inagaki, and T. Shintake, in *Proceedings of the 5th Annual Meeting of Particle Accelerator Society of Japan* (Only Title and Abstract in English) (Higashihiroshima, Japan, 2008), pp. 555–557.
- [17] A. Kawasaki, T. Aoki, A. Tokuchi, T. Shintake T. Inagaki, H. Takebe, and C. Kondo, in *Proceedings of the 5th Annual Meeting of Particle Accelerator Society of Japan* (Only Title and Abstract in English) (Higashihiroshima, Japan, 2008), pp. 565–567.
- [18] T. Inagaki, H. Baba, T. Shintake, K. Togawa, K. Onoe, H. Matsumoto, T. Takashima, A. Tokuchi, and S. Naito, in *Proceedings of APAC2004* (PAL, Pohang, Korea, 2005), pp. 654–656.
- [19] Y. Otake, H. Maesaka, T. Ohshima, N. Hosoda, T. Fukui, T. Ohata, and T. Shintake, in *Proceedings of FEL2006* (BESSY, Berlin, Germany, 2006), pp. 645–648.
- [20] Y. Otake, T. Ohshima, N. Hosoda, H. Maesaka, T. Fukui, T. Ohata, M. Musha, K. Tamasaku, M. Kitamura, K. Imai, M. Kouroggi, and T. Shintake, in *Proceedings of ICALEPCS07*, edited by Ch. Petit-Jean-Genaz (SNS-ORNL and Jefferson Laboratory, Knoxville, Tennessee, 2007), pp. 706–710.
- [21] Y. Otake, H. Maesaka, M. Kitamura, T. Shintake, T. Ohshima, N. Hosoda, T. Fukui, and T. Ohata, in *Proceedings of APAC2007* (Raja Ramanna Centre for Advanced Technology, Indore, India, 2007), pp. 634–636.
- [22] H. Maesaka, T. Ohshima, N. Hosoda, T. Fukui, T. Inagaki, S. Takahashi, T. Hasegawa, S. Tanaka, M. K. Kitamura, Y. Otake, and H. Tanaka, in *Proceedings of the 5th Annual Meeting of Particle Accelerator Society of Japan* (Only Title and Abstract in English) (Higashihiroshima, Japan, 2008), pp. 530–532.
- [23] H. Maesaka, T. Ohshima, N. Hosoda, T. Fukui, T. Inagaki, Y. Otake, H. Tanaka, S. Takahashi, T. Hasegawa, S. Tanaka, and M. K. Kitamura, in *Proceedings of the 11th European Particle Accelerator Conference*, edited by I. Andrian, O. Brüning, Ch. Petit-Jean-Genaz, and P. Pierini (INFN, ELETTRA, Sincrotrone Trieste and CERN, Genoa, Italy, 2008), pp. 1404–1406.
- [24] S. Tanaka, K. Togawa, M. Yamaga, M. Yabashi, Y. Tajiri, T. Hasegawa, T. Morinaga, Y. Kano, R. Yamamoto, Y. Otake, and H. Tanaka, “Performance Improvement of an Electron Orbit Correction System in the SCSS Test Accelerator”, *the 5th Annual Meeting of Particle Accelerator Society of Japan*, JAEA, Tokai-mura, Japan, 2009.
- [25] J. Wu and P. Emma, in *Proceedings of the 23rd Liner Accelerator Conference* (ORNL, Knoxville, TN, 1996), pp. 277–279.
- [26] Y. Tajiri, K. Togawa, M. Yamaga, H. Maesaka, M. Yabashi, S. Tanaka, T. Hasegawa, T. Morinaga, Y. Kano, R. Yamamoto, Y. Otake, and H. Tanaka, “Energy Feedback for SASE-FEL Stabilization in SCSS Test Accelerator”, *the 5th Annual Meeting of Particle Accelerator Society of Japan*, JAEA, Tokai-mura, Japan, 2009.
- [27] D. X. Wang, G. A. Krafft, and C. K. Sinclair, *Phys. Rev. E* **57**, 2283 (1998).
- [28] M. Nagasono, private communication.